Thermally-resilient image sensor packaging approach for Mars2020 Enhanced Engineering Cameras

Colin McKinney, Timothy Goodsall, Reza Ghaffarian, Richard Blank, Michael Blakely, Anupam Choubey, and Sean Howard

Jet Propulsion Laboratory, California Institute of Technology, 4800 Oak Grove Dr., Pasadena, CA 91109
Colin.McKinney@jpl.nasa.gov, Timothy.Goodsall@jpl.nasa.gov, Reza.Ghaffarian@jpl.nasa.gov, Richard.Blank@jpl.nasa.gov, Michael.J.Blakely@jpl.nasa.gov, Anupam.Choubey@jpl.nasa.gov, James.S.Howard@jpl.nasa.gov

Abstract— **Electronics designed for NASA planetary missions such as the Martian surface environment require wide-temperature survivable electronics packaging designs to ensure high-reliability avionics and instrumentation. Planetary surface temperature range of -135C to +40C dictate that electronics packaging solutions provide resiliency to large thermal excursions to counteract mismatches in the coefficient of thermal expansion in the myriad of materials found within space born electronics.**

The Mars2020 Enhanced Engineering Cameras (EECAMs) are a collection of medium- and wide-angle cameras used across the Mar2020 Flight System. The EECAMs use a commercial off the shelf (COTS) image sensor [1] packaged in a 143-pin Ceramic Pin Grid Array (PGA). Early in the EECAM development, breadboard camera electronics that used conventional thru-hole soldering techniques was subjected to limited thermal cycling to investigate packaging survivability in Martian surface thermal environments from -135C to +70C. Functional testing following 2000 cycles showed that the detector was inoperable. Visual inspection of the part exhibited sever solder joint cracking in a substantial number of pins, and in some cases resulted in complete sheering of the pins from the ceramic package substrate.

We will present the steps taken to derive the thermally-resilient electronics packaging design of the Mars2020 EECAM detector. We will highlight analyses and empirical test results that lead to a wide-temperature-survivable COTS component packaging design. Details of thermal cycle testing, in-process inspections, and final packaging design will be presented.

TABLE OF CONTENTS

1. This work was carried out at the Jet Propulsion Laboratory, California Institute of Technology, under a contract with the National Aeronautics and Space Administration.
2. 978-1-5386-6854-2/19/$31.00 ©2019 IEEE

1. INTRODUCTION

The EECAMs are a new development for the Mars2020 mission and provide significant improvements for engineering functional imaging and surface productivity use cases when compared to heritage MSL Engineering cameras. The EECAMs provide imagery essential to basic Flight System engineering functions such as rover driving, arm placement, wheel inspection, drill assessment, drilled sample assessment, rover attitude determination, and rover deck imaging. A total of nine EECAMs will be used across the Mars2020 Flight System for varying imaging use cases. Eight of these cameras are configured as four stereo pairs and are used to create stereoscopic image meshes used primarily for in-situ blind drive, auto-navigation, robotic arm workspace imaging, and rover localization operations. Additionally, the rover's Sample Caching System (SCS) intends to use an EECAM to document sample tube operations.

2. EARLY PACKAGING FAILURES

In 2014 a risk-reduction effort began to develop a prototype EECAM with flight-like electronics and subject it to thermal cycle testing. This test intended to expose the electronics (with detector installed) to a wide range of temperatures expected on the Martian surface and investigate the resiliency of the electronics packaging design. Mission environmental requirements dictate that the camera electronics must survive three times the mission lifetime (1005 Martian Sols), or 3015 total thermal cycles resembling the day to night thermal swings experienced during the mission. An accelerated test was chosen to shorten the amount of time taken to perform the thermal cycling, while limited the rate of change of temperatures to 5°C.

During inspections at the equivalent of 2X mission life, stress fractures on the detector package were observed in two locations: a) between the pins and brazed join on the package ceramic and b) at the solder joints on the Printed Circuit Board (PCB). Further, electrical tests at this inspection point showed loss of detector function. This failure mode is due to fatigue from thermally

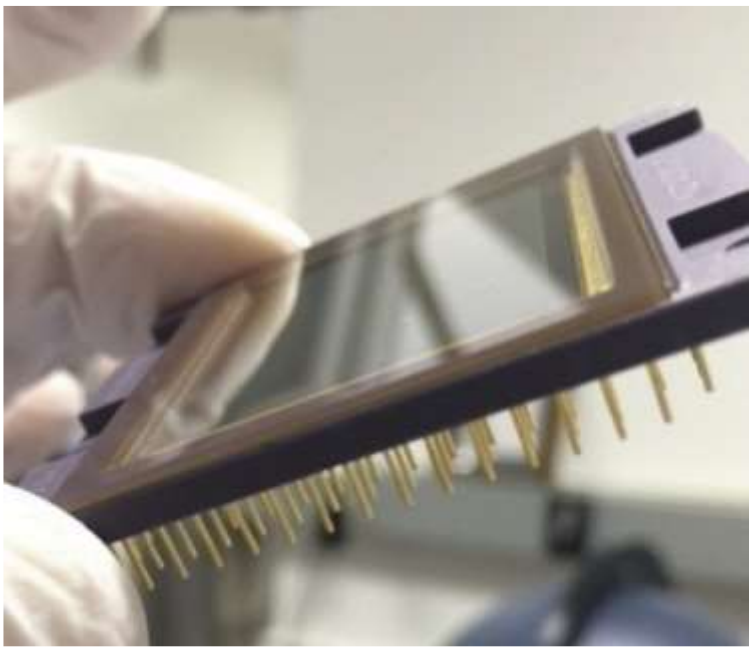

Figure 1. Image of CMV20000 detector in PGA-143 package

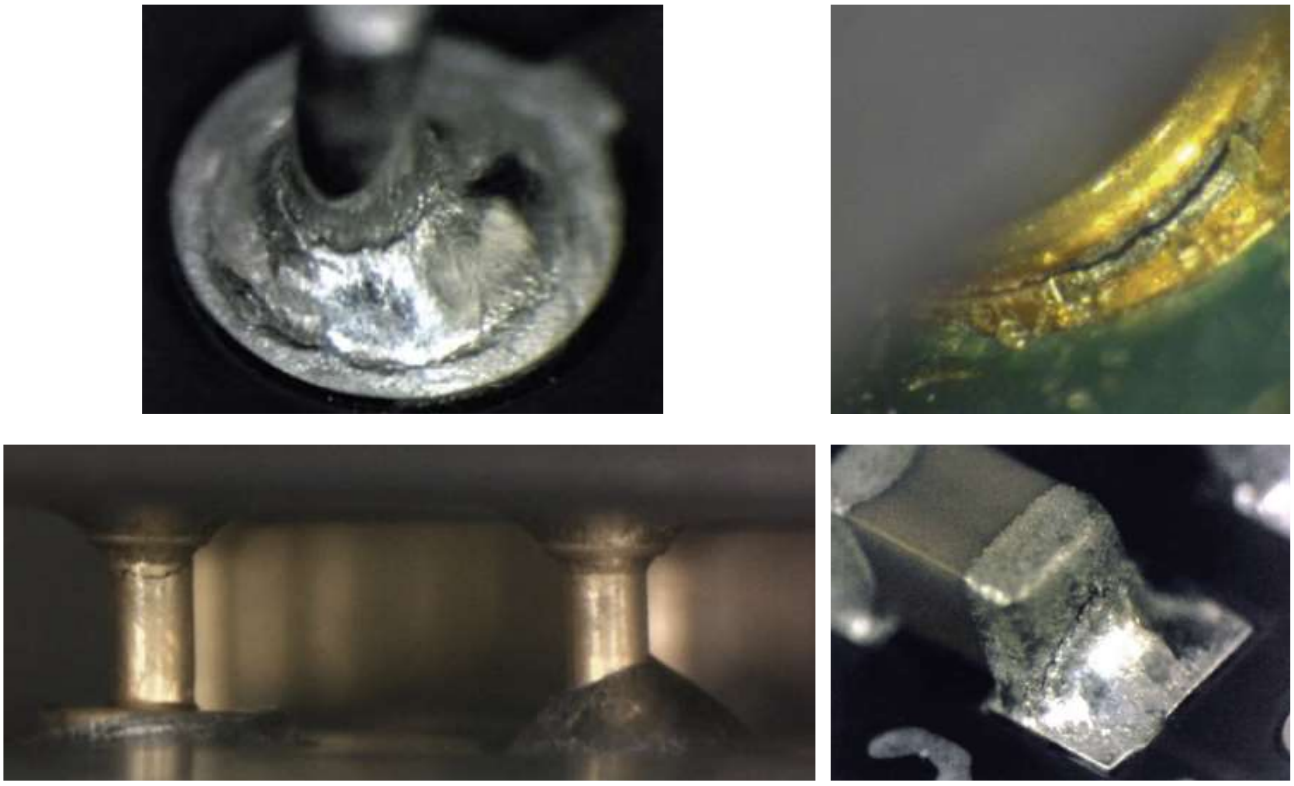

Figure 2. Various stress fractures on detector package pins (top left, top right), solder joints (bottom left), and passive components (bottom right)

induced stresses between the detector package and PCB, and between the package pins and the solder joints within the PCB (i.e in the through-hole solder junction). Figure 1 shows an image of the detector package.

Figure 2 shows a number of pictures from the inspection report detailing the various stress fractures on package pins and solder joints (on both pins and passive components).

A contributory factor in the original assembly package failures was the accelerated thermal profile used for the testing (using a 205°C temperature range). The extended

temperature range and greater extremes likely led to an overstress of the parts and exacerbated the stress-induced fatigue.

3. THERMAL PROFILE CHANGES TO REFLECT EXPECTED ENVIRONMENTS

To mitigate this failure, a second round of thermal cycling was conceived to demonstrate that changes to how the detector package mounts to the PCB assembly could eliminate these failure modes over the 3x thermal cycling period. In addition, the environmental testing profile was modified so as not to overstress the assemblies during test. Rather than revert to the standard M2020 Package Qualification and Verification (PQV) thermal cycling requirements in the Environmental Requirements Document (-135°C to +70°C), a new set of thermal cycling parameters were approved by flight system management that narrowed the temperature delta on the parts to reflect predicted temperatures of the hardware on the surface of Mars. These new temperature deltas use less pessimistic thermal modelling of the environment for the cameras. The new temperature cycling reduced the temperature range in all seasons and introduces a new winter season with much reduced temperature swings. The total number of cycles is still 3015 per the 3X Martian life requirement (a Martian year is 670 days and the mission lifetime 1.5 years, equating to ~1000 cycles per 1X lifetime). Table 1 below shows the temperature ranges used in the original risk-reduction temperature cycling; the nominal M2020 PQV requirements from the M2020 Environmental Requirements Document (ERD); and the new seasonal cycles developed for this temperature cycling.

Table 1. Temperature cycling profiles used in risk-reduction exercises

Cycle	Season	Low (°C)	High (°C)	ΔT (°C)	No. Cycles
Accelerated Risk Reduction		-135	+70	205	1530
Mars2020 PQV	Summer	-105	40	145	2115
	Winter	-135	15	145	900
Modified Seasonal Cycles	Summer	-80	+50	130	2115
	Winter 1	-115	-10	105	450
	Winter 2	-110	20	130	450

4. THERMALLY RESILIENT PACKAGING APPROACHES

The original EECAM prototype soldered the detector package directly into the PCB using a 0.05” standoff height. This distance was set by collars on the corner package pins (as shown in the right panel of Figure 1). Two modifications to the assembly method were prioritized for testing and each is discussed in turn below.

Approach 1: Increased Package Standoff Height

This is a modification to the original approach of soldering the PGA package pins directly into the PCB. The change is to increase the spacing between detector package and PCB (see Figure 3). The increased exposed package pin length introduces more compliance between the ceramic package and PCB and so reduces the maximum stresses seen by the pins themselves (although as we shall see not necessarily in the solder joints). Finite element analysis (FEA) derived the expected thermally induced stresses at the maximum temperature excursions, which demonstrated that an increase in stand-off height from the nominal 0.050” (set by a tab on the corner package pins) to 0.100” would lead to a 2x reduction in the maximum stress the package pin would endure during thermal cycling. This reduction in stress will naturally lead to an increase in the lifetime of the pin.

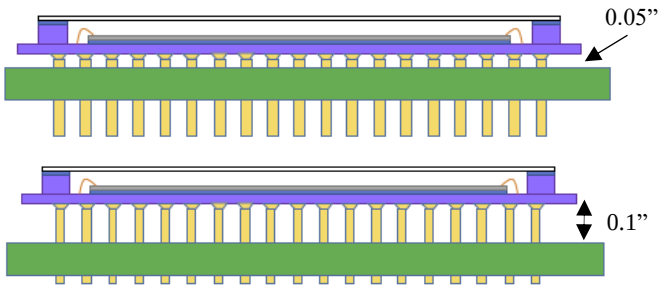

Figure 3. Illustraion of nominal (top) and increased-standoff (bottom) height between detector and PCB

One of the difficulties inherent to FEA is that the analysis is only as accurate as the materials and model data assumed. Predicting the absolute values of stress and strain the assemblies will see during thermal cycling is challenging. However, it is possible to perform analyses with different model parameters, in this case different standoff heights, and safely make comparative predictions.

Detailed data on the fatigue lifetime of the Kovar package pins was not available (let alone over the full thermal cycling temperature range) for modelling. An external company was contracted to perform fatigue measurements on the package pins to determine room temperature life and Kovar yield strength behavior. This would have been very beneficial in predicting the outcome of the thermal cycling test based on the FEA. Unfortunately, due to limitations in the test capability the measurements could not directly transfer to the current analysis (thermal cycling of bonded parts leads to reproducible displacement during thermal cycling rather than repeated stress levels. Typically, fatigue testing is designed to replicate the latter rather than the former). Nevertheless, the comparative predictions made it clear that maximizing the standoff height between detector package and PCB would reduce the chance of fatigue failure in the package pins. Increasing the standoff height beyond 0.100” with standard PCB thickness of 0.062” was not possible without having the package pins flush, or only partially inserted, into the PCB through-holes. Figure 4 shows results of ¼ FEA of the detector package at different standoff heights.

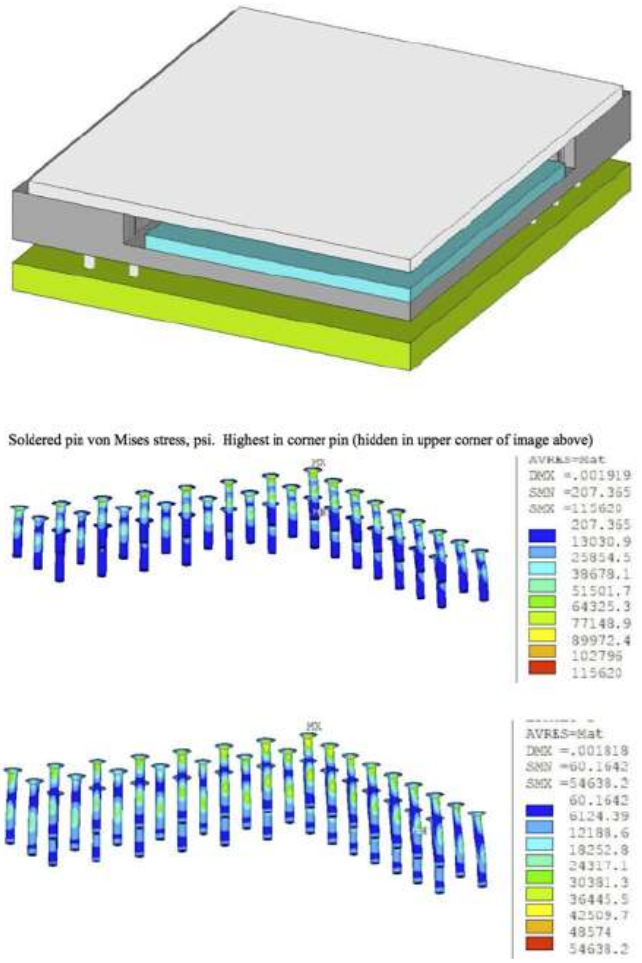

Figure 4. Top - ¼ FEA model of package and PCB assembly. Middle/bottom - 2X reduction in pin stresses from 0.05" to 0.1" height at +100°C from zero stress point.

To add further to the standoff height, fabricating a thinner (0.047") PCB would provide an additional 0.015" of standoff height over the already increased 0.100". Rerunning the analysis with the thinner PCB showed a linear relationship between standoff height and maximum stress. Increasing the standoff distance by an additional 15% would reduce the chance of fatigue failure even further, and reduced the maximum predicted stresses below published values for Kovar yield stress. The nominal test assembly consisted of an 8--layer PCB fabricated with a thickness of 0.062" with 0.024" diameter through holes. A variant with 0.030" diameter through holes were manufactured as well to determine if there was an optimum solder wall thickness that provides for more compliancy without reducing the overall strength of the solder joint. Previous work had shown that a solder wall radial thickness of 0.003" provided the optimal joint strength. With a 0.018" diameter pin, a 0.024" thru-hole diameter would deliver the 0.003" radial solder thickness. However, to survive the thermally induced stresses there was some uncertainty whether a less stiff and more compliant solder joint would have a greater lifetime. An increased through-hole diameter of 0.030" was chosen to test this hypothesis.

Approach 2: Jumper Wire Approach

The Jumper Wire approach eliminates the through-hole solder joint and resembles a common 'dead-bug' electronic packaging approach common in the aerospace industry. Instead of soldering the pins into the plated thru-holes of the printed circuit board, the pin is allowed to float freely in the thru-hole and a loop of wire is soldered to the tip of the package pin and then bent around for attachment to a bond pad on the surface of the PCB. Figure 5 below shows close up photos of the PCB test article and the jumper wire solder joint (taken during inspections). This approach eliminates the stiff mechanical constraint between the pin and PCB. The pin is left floating inside the PCB thru-hole and instead the differential thermal motions are soaked up by the much more compliant jumper wire. In this configuration, the jumper wire is never subjected to stresses exceeding the yield stress of the wire material and the corresponding fatigue lifetime was expected to far exceed the 3X margin applied during thermal cycling. This approach has been used before on Mars Science Laboratory (MSL) [2] (e.g. Cold-Encoder) and has proved itself out in a Martian environment.

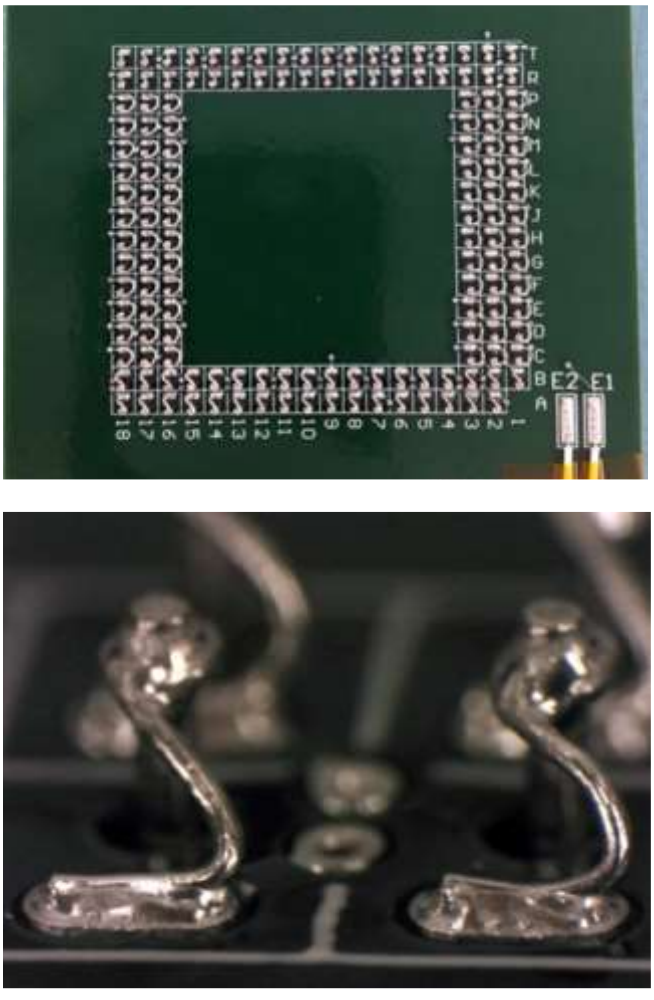

Figure 5. Jumper-wire soldered to floating package pin and soldered to a surface-mount pad on the PCB.

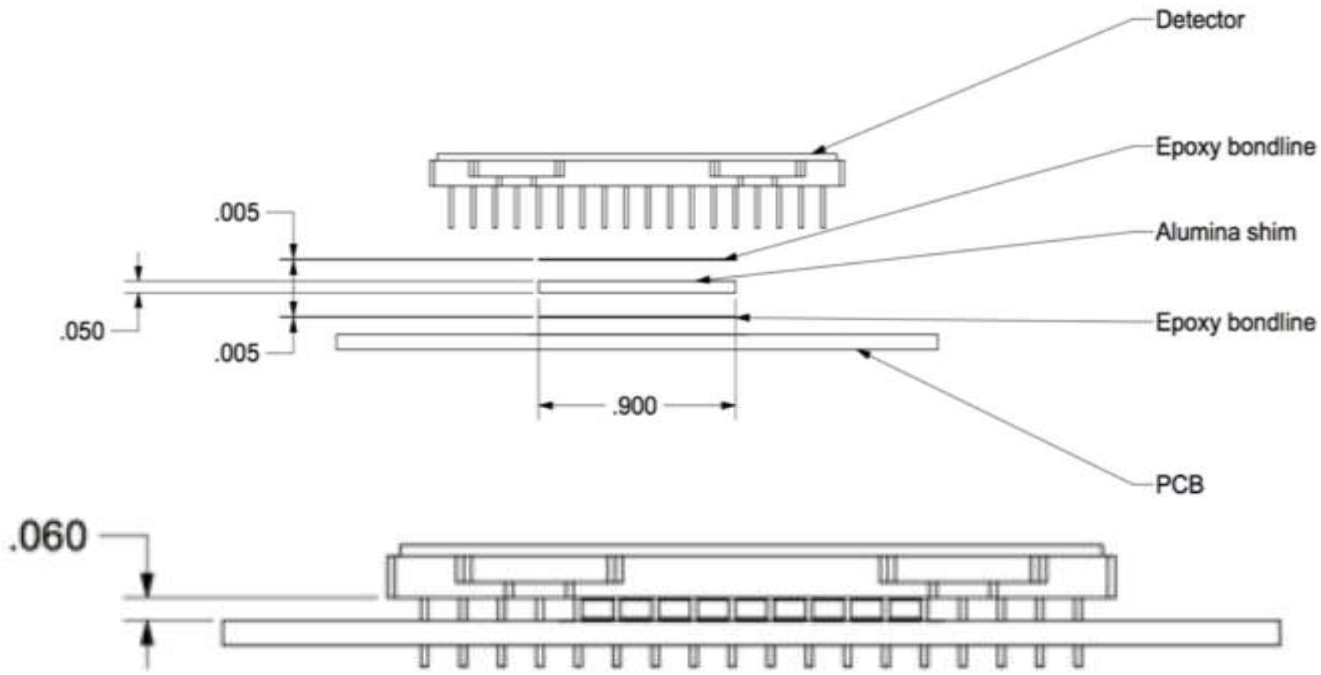

Figure 6. Packaging for jumper wire approach, dimensions in inches

Within this configuration two styles of wire-loop were tested (with an approximately equal number on each test board), which can both be seen in the top panel of Figure 5. One is a simple U-shaped loop, the other a S-shaped loop. The purpose of two shapes was to test if there was any difference between the two at 3X life. Both solutions proved equally resilient to thermal cycle fatigue, and the S-shaped loop shall be used for future assemblies.

To mechanically fix the detector package to the PCB a ceramic shim was epoxy bonded between the package and PCB (see Figure 6). Two epoxies suitable for space applications were tested for the bonds – 3M 2216 & Hysol 9309. Both have been used in the thermal environments to which the hardware will be subjected. 9309 is known to have especially good properties at low temperature and would be preferred for the expected thermal environments of the cameras. As the epoxy bond was an additional factor in the jumper wired bond additional test coupons were fabricated to test the reliability of the epoxy (results discussed later).

5. SECOND THERMAL CYCLE TEST

Ten assemblies with the soldered pins (Qty. 5 with .024" holes and Qty. 5 with .030" thru holes) and two assemblies with the Jumper Wires were fabricated for a second round of thermal cycling. Of the two primary assembly configurations, seven of the ten solder pin boards reached 3X along with both jumper-wired boards. Fewer jumper-wired samples were tested as each jumper wire represented an individual test sample of the technique.

Packaging engineers within JPL worked to manufacture the assemblies. The test assemblies were configured to provide continuous monitoring of the hardware during thermal cycling. This was achieved by forming a series resistance tracing a path through all the package pins via traces in the PCB and wire-bonds on the detector package. Further details are in the appendix. JPL electronics fabrication performed the wire-bonding of ceramic packages and carried out the epoxy bonding of dummy detector silicon die to the package.

Figure 7 shows several test assemblies installed on an aluminum fixture in the environmental chamber. The fixture allowed stacking of test assemblies in two levels. Each assembly was connected to a data logger which provided continuous series resistance measurements. These were inspected on a daily basis and any anomalies reported.

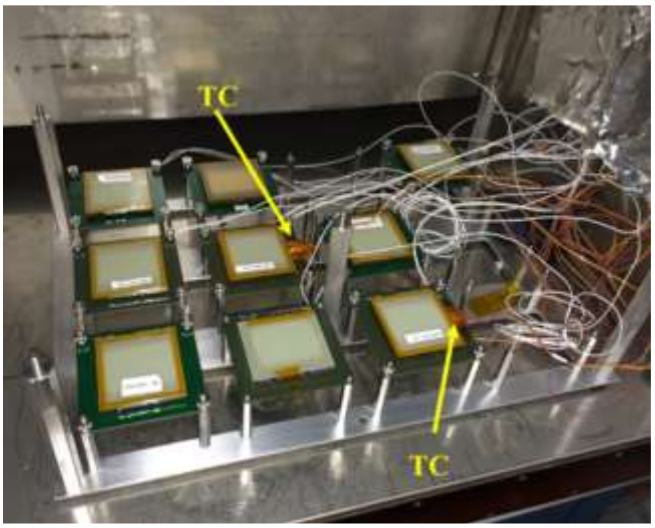

Figure 7. Second round thermal cycle test assemblies wired for in-situ series resistance measurements

The failure criteria for the test was defined as any increase in daisy chain resistance greater than 20% (after accounting for thermally induced resistivity changes).

Thermal cycling began on 2016-04-12 and was completed on 2016-12-08. The average number of cycles completed each day was approximately 15. The total cycling time was roughly 200 days with the additional 40 days taken up by inspections, servicing of the environmental chambers etc.

After approximately one week of cycling, three anomalies were detected in the thermal cycling data. As the temperature of the chamber dropped below -20°C the daisy--chain resistance on three test assemblies (#s 26, 28 & 45) jumped up by roughly 30 ohms before continuing to track the temperature change. On warming to above -20°C the resistance dropped back to about 10 Ohm before once again tracking the temperature. This was determined to be due to a wire-bond on the package shorting out a large fraction of the daisy-chain. As the temperature of the chamber dropped the short opened and the "normal" high series resistance was restored. More details are available in the appendix.

Figure 8 shows an example of continuous monitoring data from a sample of assemblies. The assemblies with mean resistance of around 10 Ohms have packages with the short described above. However, the short does not open or close as the temperature changes. The high mean value of around 40 Ohms corresponds to the expected series resistance without the short. One assembly is discrepant due to a short in a different location.

It was determined that this package short affected half of the soldered pin assemblies. Rather than repair the wire-bond shorts it was decided to leave them in place until completion of thermal cycling. After 3X inspections the shorts were removed and the affected packages returned to the chamber for 16x cycles.

The series resistance followed the expected trend with temperature and showed no anomalous behavior and matched the results for the other test assemblies unaffected by the package short.

6. Inspections and Test Results

After eight months of thermal cycle testing, in-process inspections, and anomaly debugging, the second thermal cycle test was completed. Aside from the anomalous resistance measurements seen in three boards, no board met the fail criteria at any point during 3X thermal cycles.

Soldered Pin Assemblies

At each inspection point the pins and solder joints for each test assembly were carefully assessed. Howard recorded his inspection results by drawing maps of fracturing in the package pins. These maps were updated at each inspection point to show the additional fractured solder joints observed. Figure 9 shows a fracture map for one test assembly. The shapes show the additional fractures that developed at each successive inspection point. It can clearly be seen that the initial fractures developed at the outer edges and corners of the assembly. As the number of thermal cycles accrued the inner pins began developing fractures. By 3X nearly all the pins on the assembly had developed a fracture in the solder joint.

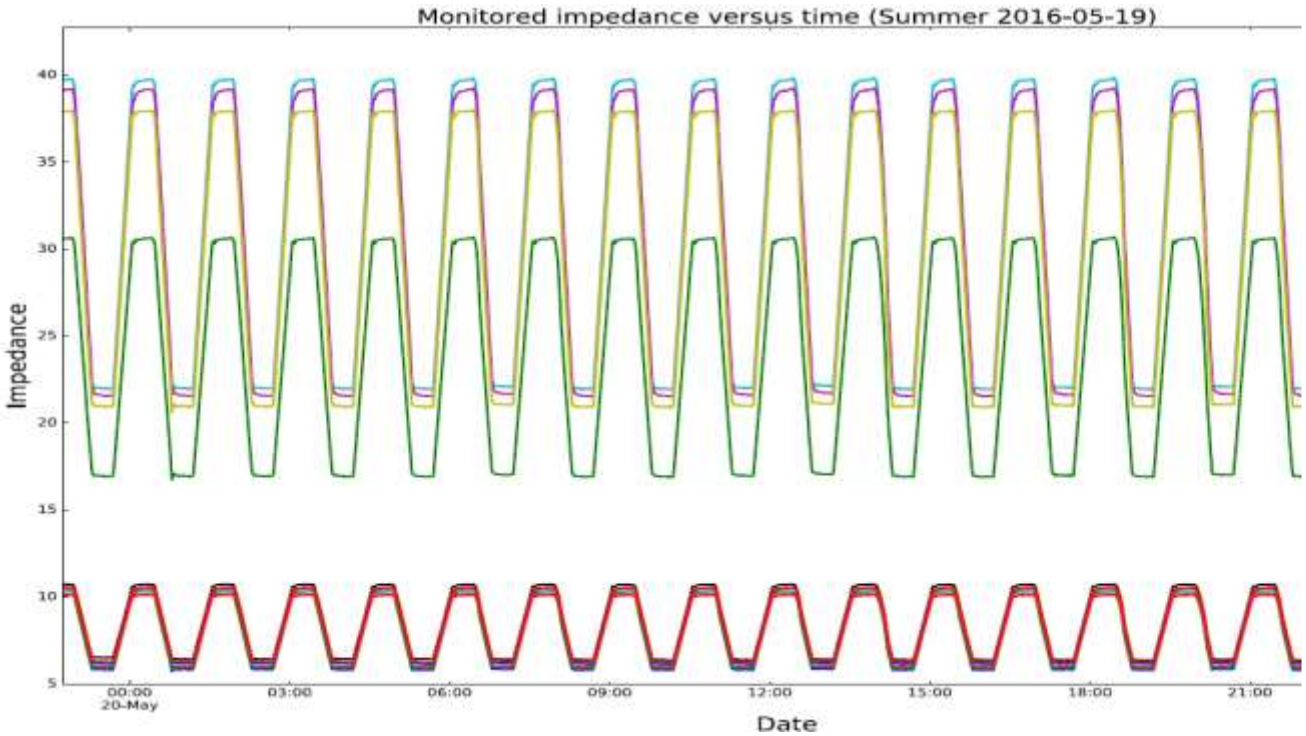

Figure 8. Plot of individual test assembly package daisy-chain resistance over temperature vs. time.

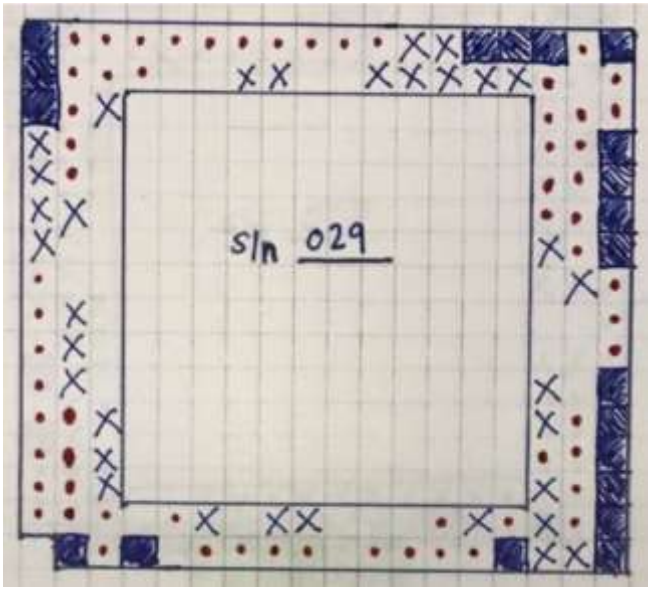

Figure 9. Solder joint fracture map. Squares = 1X life, circles = 2X life, and X = 3X life occurrence

No evidence of stress lines or any fracturing in the package pins was found at any stage on any of the soldered pin assemblies. This validates the FEA model showing increased pin height reduces thermally induced stress on package pins. At 1X life inspections of the soldered pin assemblies made with 0.047" thick PCBs showed no evidence of any solder joint fracturing.

Figure 10 and Figure 11 show inspection photos (from the 3X report) of solder joint fracturing on the underside and topside of the assembly respectively.

Figure 10. Radial and annular fracturing on the solder joint, bottom side of PCB

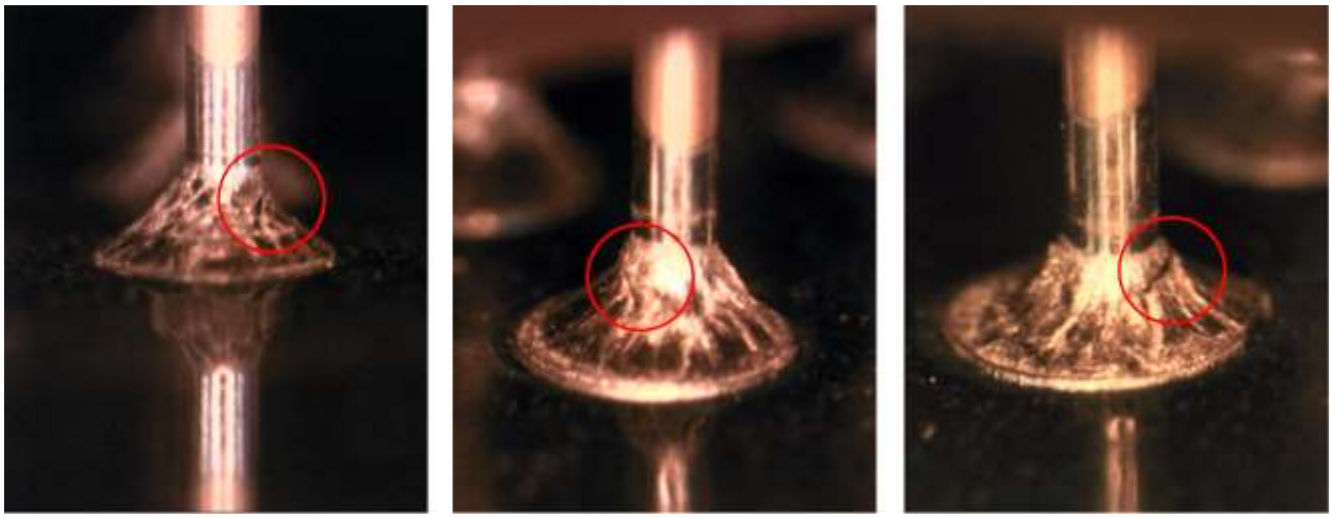

Figure 11. Micro-fractures on the package pin solder joints, highlighted by red circles.

Jumper Wire Assemblies

At 3X the jumper wired assemblies showed only nominal signs of age seen via increased granularity in the solder joint at the tip of the package pins. This is illustrated in Figure 12. Otherwise the jumper wired boards looked in "as-new" condition at the end of 3000+ thermal cycles. The epoxy bonds between the PCB, ceramic shim and package sandwich showed no signs of damage from visual inspection.

Cross-sections of the epoxy test coupons, for both samples (9309 and 2216) were been performed along with acoustic microscopy. The 2216 bonded parts showed no evidence of delamination at the PCB-shim and shim-detector bonds at 3X life. The 9309 sample showed regions of cracking and delamination. Lap-sheer tests to determine the reliability of the bond proved successful and were approved as a structural bond.

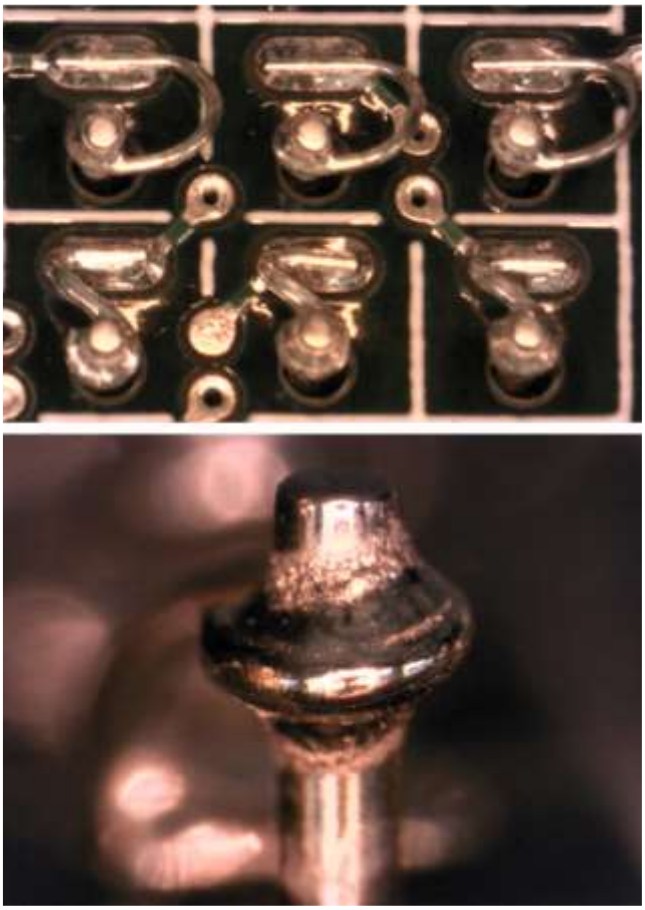

Figure 12. Jumper-wire solder joints after 3X life

7. Destructive Physical Analysis

Several destructive parts tests were carried out post 3X inspections for the soldered-pin assembly boards. Cross-sectioning of a sample of the soldered pin boards was performed to determine the extent of fracture propagation. After completion of 3X inspections two of the soldered pin boards (#29 and #43) were selected for cross-sectioning to determine the extent of the fracture propagation into the PCB through-hole. These cross-sections provide important additional information as to the expected reliability of the solder joints. While the failure criteria had not been met during testing the visual inspections raised serious doubts about the reliability of the solder joints. Cross-section analysis of a sample of boards to determine the depth of fracture propagation into the solder through holes is necessary to provide a much better handle on the proximity to failure.

Figure 12. Cross-section analysis reference for soldered pin SN #29

The JPL Analysis and Test Laboratory (ATL) carried out the cross-sectioning of the two aforementioned soldered pin samples. They were chosen by selecting the two boards which had the greatest and fewest number of fractures on the solder joints (however the board to board spread was not significant). Figure 12 shows a map identifying the cross--section locations. Figure 13 shows example fractures from #29. The first two are for side A at each end and the third from side B. As can clearly be seen the fractures propagate only a small distance into the solder barrel of the PCB. This indicates the thru-holes are not likely to fail imminently. However, it would be unwise to attempt to predict the future life the thru-holes may have.

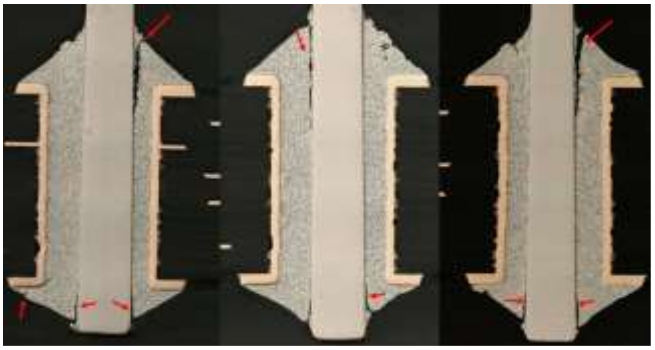

Figure 13. Cross-sections of soldered pins on SN #29.

The cross-section does preclude seeing the full 3D geometry of the fracture, but given the section completely cuts across the pin diameter it is unlikely the fracture propagation extends significantly further down out of plane of the section.

There is evidence that the 0.024” diameter holes mitigate the level of fracture propagation into the solder barrel and should be the baseline dimension for future detector assemblies of soldered-pin type.

8. SUMMARY

Following extensive piece-part analysis, thermal cycle testing, and destructive parts analysis, the Mars2020 Enhanced Engineering Camera task explored thermally-resilient packaging techniques for the CMOS detector within the camera.

All test samples of the increased-height soldered pin and jumper-wire configurations passed 3X life thermal cycles of the Mars2020 temperature cycle requirements. DPA results identified near-failure conditions of the package solder joints, and therefore the jumper-wire approach was chosen to be the baseline for the camera packaging design. The overall health and resiliency of the jumper-wire solder joints inspired confidence that this packaging approach would best serve the cameras well beyond their planned operational life on Mars.

9. APPENDIX

Early anomalies in the thermal cycling were found on three of the original 12 test articles. These parts were removed from thermal cycling for closer examination. The anomaly, as shown in Figure 14 below, manifested as an increase in daisy-chain series resistance as the test article temperature decreased. After reaching the bottom of the thermal cycle and on return to room temperature, the series resistance dropped again. The initial determination was that this was due to a loose wire-bond. For one of the test articles the daisy-chain wire-bonds on the detector package were re-worked to add a second bond alongside the existing ones. This failed to address the problem. It was then mooted that a flaw existed in the package fabrication leading to a short in the daisy-chain that opened when the material temperature dropped below some threshold.

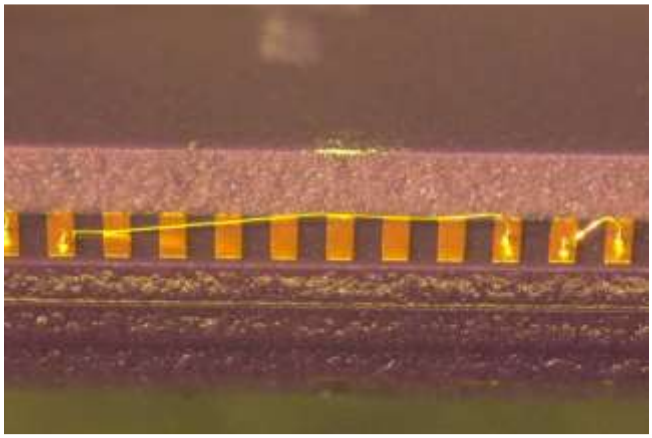

Figure 14. Micro-scope image of wire-bond short across long bond length. Short present on left side of image, on pad adjacent to bond.

After a detailed investigation and measurement of the series and point-to-point resistances in the daisy-chains of the packages the exact location of the short was identified. The short was roughly 1/3 of the way around the daisy-chain from the ‘start’ and shorted the chain directly to the end – which was also detector package ground.

The daisy-chain called for some wire-bonds on the detector package bond pads that stretched over multiple bond pads. One particular bond was placed such that at the wedge end of the bond the wire grazed a neighboring bond pad. This neighboring pad happened to be the package ground plane connection.

During cooling the change in shape of the wire due to thermal contraction led to it lifting off the surface of the ground-plane bond pad causing the daisy-chain to exhibit normal series resistance. The short caused by this grazing incidence wire-bond was not replicated in all the test articles.

The assemblies under test were not re-worked to repair this short between the 2X and 3X inspection points to avoid adding in additional variables into the test. However, at completion of 3X cycles the five test samples which were affected by the short were returned for repair. An engineer affected the repair by gently lifting the wire-bond at the wedge end to remove the short. The five repair assemblies were then returned to the environmental chamber for an additional 15 cycles to measure the at-temperature daisy-chain resistance to determine if any opens had occurred. The results confirmed that no opens occurred which were masked by the short in the daisy-chain.

ACKNOWLEDGEMENTS

The authors thank Rajeshuni Ramesham, Ryan Ross, and the rest of the JPL Environmental Test and Qualification Laboratory (ETQL) facility for their support and guidance during this task.

The work described in this paper was carried out at the Jet Propulsion Laboratory, California Institute of Technology, under a contract with the National Aeronautics and Space Administration.

REFERENCES

[1] CMOSIS. "CMV20000 datasheet v2.3" *cmosis.com*, AMS Sensors Belgium, 2015. Web.

[2] "Electronic Packaging Materials for Extreme, Low Temperature, Fatigue Environments." (Accepted, to IEEE Transactions in Advanced Packaging, October 2009) A.A. Shapiro, C. Tudryn, D. Schatzel, S. Tseng

BIOGRAPHY

Colin McKinney *received his B.S. degree in Electrical Engineering from Cal Poly, San Luis Obispo in 2008. He is a member of the Flight Detector and Camera Systems group at JPL, responsible for the delivery of the Enhanced Engineering Cameras for the Mars2020 Rover. He is also active in the research and development of the enabling technologies for extreme environment (wide-temperature, high radiation) visible camera systems for NASA's planetary missions to Mars and the Jovian system.*

Dr Timothy Goodsall *received his DPhil in Astrophysics, specializing in instrumentation, from the University of Oxford in 2009. He is a Technologist within the Advanced Detectors, Systems and Nanoscience group at JPL specializing in the development and characterization of detectors and instrument systems.*

Dr. Anupam Choubey *received his Ph.D. in Mechanical Engineering from University of Maryland at the Center of Advanced Life cycle engineering (CALCE) in 2007 and M.S. from SUNY Binghamton in 2003. He is currently work in Reliability Engineering and Mission Environmental Assurance group at NASA-JPL. He leads the Extreme Thermal Environment life cycle, Package Qualification and Verification (PQV) Program at JPL. He has led analysis and test efforts for JPL missions such as INSIGHT, Mars2020, OSIRIS-REX, JUNO and EUROPA. He specializes in electronics failure mechanisms and utilizes his skills, including physics of failure (PoF) and use of advanced analytical tools for anomaly investigations. He has worked at several companies prior to JPL such as Dow chemicals and Vicor corporation and played significant roles in developing processes for surface mount and Underfill for 2.5D and 3D packaging technologies. Dr. Choubey, has published a book named "Copper wire bonding" and has over 20 articles published in Journals, NASA bulletins and has 2 filed patents.*